Tectonophysics, 21 (1974): 1–13

TEMPERATURES IN A CONVECTING UPPER MANTLE

J.Cl. DE BREMAECKER

Department of Geology, Rice University, Houston, Texas (U.S.A.)

(Accepted for publication May 17, 1973)

ABSTRACT

De Bremaecker, J.Cl., 1974. Temperatures in a convecting upper mantle. *Tectonophysics*, 21: 1–13.

Numerical computations show that in a convecting upper mantle the temperature rises rapidly to about 1000°C near a depth of 100 km; below this depth it stays essentially constant until about 350 km. This result agrees with data obtained from the olivine–spinel phase change.

INTRODUCTION

Much attention has recently been paid to the phenomena which occur during the descent of a lithospheric plate through the upper mantle (Minear and Toksöz, 1970; McKenzie, 1972; Griggs, 1972). It is, however, not a priori evident that these kinematic solutions are also dynamically satisfactory. More precisely, since the temperature and the convective motion are very strongly coupled, one cannot assume one independently of the other: it is just as false to say that the temperature determines the motion as to say that it is the motion which determines the temperature. We must, thus, perforce, deal with the problem of determining the temperatures in a convecting upper mantle.

In order to obtain a preliminary answer to this question, I have found it necessary to make the following simplifying assumptions:

(1) The convective cell is two-dimensional.

(2) It extends to a depth of 600 km (Tozer, 1967); its width is between 2,000 and 4,000 km.

(3) The viscosity is Newtonian and constant.

(4) The thermal conductivity is constant.

(5) The effect of phase changes is unimportant in the convective process (McKenzie, 1969).

(6) Approximately 75% of the heat is generated internally by uniformly distributed radioactive heat sources; the rest comes from below (Clark and Ringwood, 1964).

(7) All boundaries are free of stress.

(8) The surface is at 0°C; the sides are insulated.

Attention is drawn to the fact that assumption 6 is markedly different from the one made in Rayleigh-Bénard convection (Bénard, 1901; Rayleigh, 1916): in the latter the temperature along the bottom is fixed and constant, in the present case it is neither. Thus, in

the present model, the temperatures at the bottom are obtained as a result of the computations. In many other models (e.g., Torrance and Turcotte, 1971a, b) on the other hand, the temperatures at the bottom are assumed, generally on the basis of a classical, i.e., purely conductive, solution. This does not appear self-consistent.

The present case has been studied theoretically in simplified form by Roberts (1967) and experimentally by Tritton and Zarraga (1967) with noticeably different conclusions.

The problem is solved numerically by first solving the Navier-Stokes equation with an assumed temperature distribution; the complete heat-transfer equation is then solved, and the new temperature distribution is again used in the Navier-Stokes equation.

THE NAVIER-STOKES EQUATION

Many methods are available to solve the Navier-Stokes equation. The classical one (Torrance and Rockett, 1969) uses the stream function and the vorticity; a biharmonic equation in terms of the stream function may also be used (Andrews, 1972).

I have used the Simplified Marker and Cell method (SMAC) of Amsden and Harlow (1970). In this method one first solves the Navier-Stokes equation for a compressible fluid using an arbitrary pressure distribution. Using the Boussinesq (1903, vol. 2, p.172) approximation, this equation may be written for steady-state conditions (Bullen, 1963, p.34):

$$\nu\left(\nabla^2 \tilde{V}_r + \tfrac{1}{3}\frac{\partial \theta}{\partial x_r}\right) - \frac{\partial \varphi}{\partial x_r} + X_r = 0 \qquad (1)$$

For explanation of symbols see Notation I.

NOTATION I

α	coefficient of thermal expansion
δx, δy	increments along the x- and y-axes
ζ	potential (eq. 2)
θ	divergence of the velocity field for a compressible fluid (eq. 1)
ν	kinematic viscosity
ρ	density
φ	arbitrary pressure, normally close to the hydrostatic pressure
c	heat capacity at constant volume
g	gravity
F	heat flow through the bottom of the cell
H	heat produced by radioactivity per unit volume
i	index for the x-coordinate
j	index for the y-coordinate
k	thermal conductivity
r	index, = 1 for the x-axis, 2 for the y-axis (eq. 1)
R	relaxation factor (eq. 12)
s	j-index for the uppermost zone in the cell
S	heat produced by shear heating per unit volume
T	temperature
u	horizontal velocity

NOTATION I (continued)

v	vertical velocity
V	velocity vector (incomp
$\tilde{V}$	velocity vector (compre
X	body force, normally λ

The resulting velocity field of the pressure – but non-zer taneously, after which the di propriate potential, determin

$$V_r = \tilde{V}_r - \frac{\partial \zeta}{\partial x_r}$$

It follows that:

$$\frac{\partial \tilde{V}_r}{\partial x_r} - \nabla^2 \zeta = \frac{\partial V_r}{\partial x_r} = 0$$

and thus:

$$\nabla^2 \zeta = \theta$$

which determines ζ and thus

Because of the numerical of V is close enough to zero must be repeated. For the s correct pressure distribution

THE HEAT-TRANSFER EQUA

The heat-transfer equatio

$$c\rho \frac{\partial T}{\partial t} = k\nabla^2 T - c\rho(V \cdot$$

For steady-state conditions

This equation does not e it may be viewed as yieldin in order to simplify the co ($g\alpha T/c$) in the upper mantl Moreover, it only affects t Andrews, 1972, eq. 12). S vective heat transfer (Clark ligible. As a result, thus, t tures resulting from the so

NOTATION I (continued)

v	vertical velocity
V	velocity vector (incompressible fluid)
$\tilde{V}$	velocity vector (compressible fluid)
X	body force, normally $X_1 = 0$, $X_2 = g(1-\alpha T)$

The resulting velocity field, V, has the correct vorticity – since the latter is independent of the pressure – but non-zero divergence. These two equations ($r = 1, 2$) are solved simultaneously, after which the divergence is nulled by superposition of the gradient of an appropriate potential, determined as follows. Let the correct velocity field, V, be given by:

$$V_r = \tilde{V}_r - \frac{\partial \zeta}{\partial x_r} \tag{2}$$

It follows that:

$$\frac{\partial \tilde{V}_r}{\partial x_r} - \nabla^2 \zeta = \frac{\partial V_r}{\partial x_r} = 0 \tag{3}$$

and thus:

$$\nabla^2 \zeta = \theta \tag{4}$$

which determines ζ and thus V.

Because of the numerical errors involved it is necessary to check whether the divergence of V is close enough to zero everywhere; if not a new ζ has to be computed, and the process must be repeated. For the same reason φ (in eq. 1) should be taken relatively close to the correct pressure distribution.

THE HEAT-TRANSFER EQUATION

The heat-transfer equation in the time-dependent case is:

$$c\rho \frac{\partial T}{\partial t} = k\nabla^2 T - c\rho(V \cdot \nabla T) + H + S \tag{5}$$

For steady-state conditions the left-hand side is null.

This equation does not explicitly take the adiabatic gradient into account; alternatively, it may be viewed as yielding temperatures which use the adiabat as a base line. This is done in order to simplify the computations. It may be justified as follows: the adiabatic gradient ($g\alpha T/c$) in the upper mantle is ~0.3°C/km using the parameters given in Table I; this is small. Moreover, it only affects the vertical conductive heat transfer (Jeffreys, 1959, p.288; Andrews, 1972, eq. 12). Since conductive heat transfer is generally small compared to advective heat transfer (Clark, 1969), the effect of such a small temperature difference is negligible. As a result, thus, the effect of the adiabatic gradient must be added to the temperatures resulting from the solution of eq. 5.

TABLE I

Parameters of the models (S.I. and conventional units)

	Fig.3 Model 66	Fig.4 Model 12	Fig.5 Model 22
Width $(km \cdot 10^3) = (m \cdot 10^6)$	2	3	3
Depth $(km \cdot 10^2) = (m \cdot 10^5)$	6	6	6
Coefficient of thermal expansion $(°C^{-1} \cdot 10^{-5})$	3.7	3.7	3.5
Specific gravity	3.35	3.35	3.35
Viscosity $(kg\ m^{-1} sec^{-1} \cdot 10^{20}) = (poises \cdot 10^{21})$	1	2	2
Heat capacity $(J\ kg^{-1}\ °C^{-1} \cdot 10^3) = (erg\ g^{-1}\ °C^{-1} \cdot 10^7)$	1.3	1.3	1.2
Thermal conductivity $(W\ m^{-1}\ °C^{-1}) = (cal\ cm^{-1}\ °C^{-1}\ sec^{-1} \cdot 2.4 \cdot 10^{-3})$	2	2	2.5
Radioactivity $(W\ m^{-3} \cdot 10^{-8}) = (erg\ g^{-1}\ year^{-1})$	3	6	8.75
Heat flow through bottom $(W\ m^{-2} \cdot 10^{-3}) = (H.F.U. \cdot 2.4 \cdot 10^{-2}) =$ $(cal\ cm^{-2}\ sec^{-1} \cdot 2.4 \cdot 10^{-6})$	0	8	12.5
Error criterion			
On u, v, Div V, ζ	10^{-3}	10^{-4}	10^{-4}
On T	10^{-4}	10^{-4}	10^{-4}

NUMERICAL METHODS

The x-axis is horizontal and designated by the index i; the y-axis is vertical upward and designated by the index j. The x-component of the velocity is u, the y-component is v.

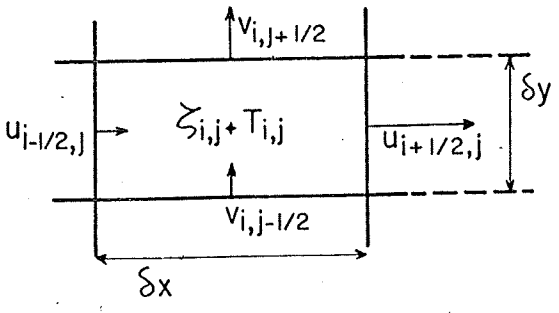

Fig.1. Placement of the variables.

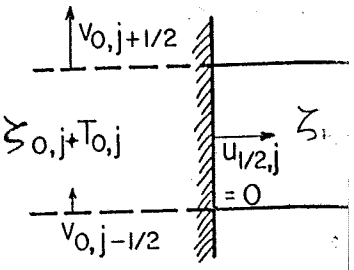

Fig.2. The variables near a boundar

The variables are placed (Fi used by Amsden and Harlow t lines will be called a zone. The by $j = s$. A fictitious row (or c putations easier; in the case si

$$u_{\frac{1}{2},j} = 0;$$

Similar conditions are used ar

Eq. 1 and 4 may be solved of successive row overrelaxa and Wasow, 1960, pp.103–1 ative root-mean-square chang tions on these quantities are same convergence criterion. less than 10^{-3} (or 10^{-4}) × v the shortest time needed for

The heat transfer equation ditions. In the case shown in

$$T_{0,j} = T_{1,j}$$

At the bottom:

$$T_{i,0} = T_{i,1} + (F/k) \cdot \delta y$$

Near the surface:

$$T_{i,s+1} = -T_{i,s}$$

so that the surface, at $j = s +$

The method of solution is In the time-dependent case Peaceman, 1966, pp.105–1 forward. The advective term

Fig.4 Model 12	Fig.5 Model 22
3	3
6	6
3.7	3.5
3.35	3.35
2	2
1.3	1.2
2	2.5
6	8.75
8	12.5
10^{-4}	10^{-4}
10^{-4}	10^{-4}

-axis is vertical upward and
. the y-component is v.

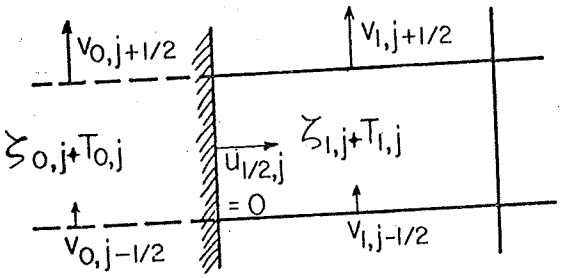

Fig.2. The variables near a boundary.

The variables are placed (Fig.1) as in Welch et al. (1966). This placement has also been used by Amsden and Harlow (1970) and by Andrews (1972). The area between the mesh lines will be called a zone. The uppermost zone inside the convective cell will be designated by $j = s$. A fictitious row (or column) is introduced outside each boundary to make the computations easier; in the case shown in Fig.2:

$$u_{½,j} = 0; \qquad \zeta_{0,j} = \zeta_{1,j}; \qquad v_{0,j+½} = v_{1,j+½} \tag{6}$$

Similar conditions are used at other boundaries.

Eq. 1 and 4 may be solved by a variety of numerical methods. I have used the method of successive row overrelaxation (S.R.O.) and the tridiagonal algorithm (T.D.A.) (Forsythe and Wasow, 1960, pp.103–105 and 266–271; Peaceman, 1966, pp.66–69). When the relative root-mean-square change on $\tilde{u}$ and $\tilde{v}$ falls below 10^{-3} or 10^{-4} (see Table I), the iterations on these quantities are terminated, and the same process is repeated for ζ using the same convergence criterion. The test for approximate nullity of the divergence is that it be less than 10^{-3} (or 10^{-4}) × volume of each zone (i.e., $\delta x \times \delta y$) in a time interval equal to the shortest time needed for any particle to traverse a zone.

The heat transfer equation (eq. 5) is then solved taking into account the boundary conditions. In the case shown in Fig.2:

$$T_{0,j} = T_{1,j} \tag{7}$$

At the bottom:

$$T_{i,0} = T_{i,1} + (F/k) \cdot \delta y \tag{8}$$

Near the surface:

$$T_{i,s+1} = -T_{i,s} \tag{9}$$

so that the surface, at $j = s + ½$, be at 0°C.

The method of solution is different for a time-dependent case and for a steady-state case. In the time-dependent case the Crank-Nicolson method (Forsythe and Wasow, 1960, p.142; Peaceman, 1966, pp.105–108), S.R.O. and T.D.A. are used. The method is long but straightforward. The advective term is written (Welch et al., 1966, p.38) in conservative form:

$$V \cdot \nabla T = [(uT)_{i+\frac{1}{2},j} - (uT)_{i-\frac{1}{2},j}]/\delta x + [(vT)_{i,j+\frac{1}{2}} - (vT)_{i,j-\frac{1}{2}}]/\delta y \quad (10)$$

where, for example:

$$(uT)_{i-\frac{1}{2},j} = \tfrac{1}{2}u_{i-\frac{1}{2},j}(T_{i-1,j} + T_{i,j}) \quad (11)$$

δt is chosen so that the fastest moving particle traverses only a fraction, f, of the zone during this interval. The best compromise between computational speed and accuracy appears to be $f = 0.4$.

In the steady-state case the conventional method of taking differences does not yield a diagonally dominant equation (Forsythe and Wasow, 1960, p.181). In order to obtain such an equation, "upwind" differences are used. This term was first used by Isaacson (Forsythe and Wasow, 1960, p.397), but the method has been rediscovered since (Greenspan, 1968, pp.122–147; Torrance and Rockett, 1969). The name is due to the fact that the temperatures at each point are differenced "upwind" (or upstream) from that point. Some care is necessary because u and v are not defined at the center of the zone. The equation is also solved by S.R.O. and T.D.A.

After convergence (convergence criterion 10^{-3} or 10^{-4}) the new temperatures T^* are combined with the temperatures of the previous iterate $T^{(k)}$ in an under-relaxation scheme to obtain the $k + 1$ iterate:

$$T^{(k+1)} = T^{(k)} + R(T^* - T^{(k)}) \quad (12)$$

where R is the relaxation factor.

The $k + 1$ iterate is then used in the Navier-Stokes equation, and the whole process is repeated until no appreciable changes occur after a complete iteration, i.e.:

$$T^{(k)} \cong T^{(k+1)}$$

Some care is necessary in choosing R; the optimum value appears to vary between 0.8 and 0.1. It may be noted that this method does not guarantee an exact steady-state solution, which in fact may not exist, but only one which fluctuates only slightly.

RESULTS

All the computations were made with the depth divided into eight equal intervals, and the width into fifteen. The depth was always taken as 600 km but the width varied from 2,000 to 4,000 km. (The middle of the top zone is thus at depth of 37.5 km.)

Time-dependent solutions

As remarked by Foster (1969) it is not possible to choose entirely realistic initial conditions; the method is, however, useful in excluding impossible ones. In particular, a series of experiments confirm that any model with a highly super-adiabatic gradient is unstable: such a gradient always produces a convective overturn accompanied by extremely high (sev-

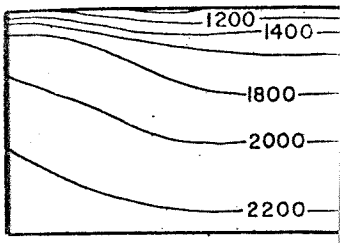

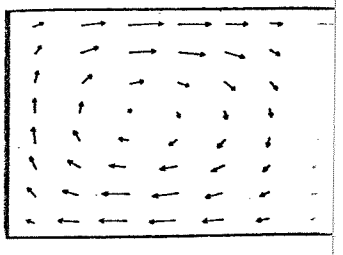

Fig.3. Temperature and velocity g gradient.

eral m/year) surface velocities was predicted by Elsasser (19 shows the results of such an e ature distribution was fairly c (3.3°C/100 km). The parame two vortices have developed continue to increase with tim in the middle of the cell, foll

The impossibility of main the constitutive relation for came greater (than adiabatic) the temperature adiabatically by viscosity, cooling at the to Clearly, this reasoning applies

These experiments also sh convect as a single cell for an parameters of the system and the convective system is real stated.

Steady-state solutions

Two typical results are sh

$_2]/\delta y$ (10)

(11)

raction, f, of the zone dur-
peed and accuracy appears

fferences does not yield a
31). In order to obtain such
used by Isaacson (Forsythe
d since (Greenspan, 1968,
the fact that the tempera-
n that point. Some care is
one. The equation is also

new temperatures T^* are
an under-relaxation scheme

(12)

and the whole process is
eration, i.e.:

pears to vary between 0.8
an exact steady-state solu-
s only slightly.

eight equal intervals, and
ut the width varied from
h of 37.5 km.)

tirely realistic initial condi-
nes. In particular, a series
batic gradient is unstable:
nied by extremely high (sev-

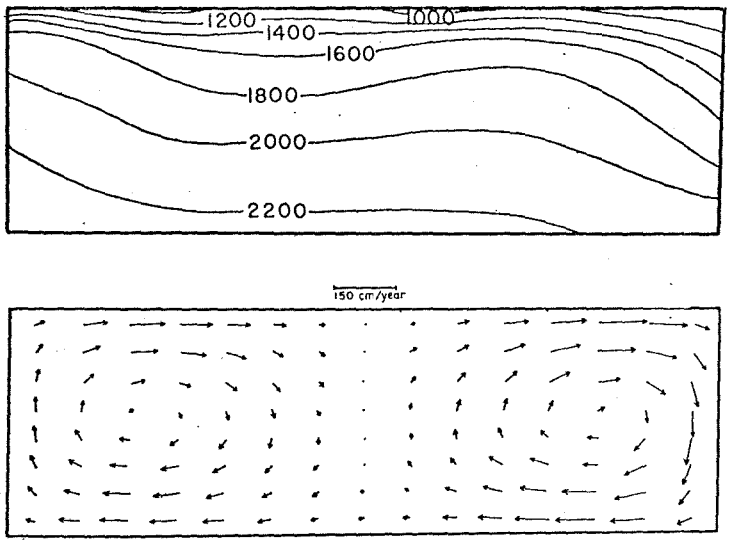

Fig.3. Temperature and velocity fields for Model 66 after $70 \cdot 10^6$ years starting with a super-adiabatic gradient.

eral m/year) surface velocities. This stage is followed by a long quiescence. This behavior was predicted by Elsasser (1966), and explains the results of Shimazu et al. (1967). Fig.3 shows the results of such an experiment (Model 66) after $0.9 \cdot 10^6$ years; the initial temperature distribution was fairly conventional, but with a slight lateral temperature variation (3.3°C/100 km). The parameters of the models are listed in Table I. The figure shows that two vortices have developed, and that surface velocities exceed 1 m/year. These velocities continue to increase with time, and after an additional 75,000 years a third vortex develops in the middle of the cell, followed by a rapid convective overturn.

The impossibility of maintaining a super-adiabatic gradient is essentially independent of the constitutive relation for, as pointed out by Jeffreys (1959, p.288) "if (the gradient) became greater (than adiabatic) convection currents would increase in vigour and redistribute the temperature adiabatically. If it became less, convection currents would be damped down by viscosity, cooling at the top would become more rapid, and the gradient would steepen". Clearly, this reasoning applies to all likely constitutive relations.

These experiments also showed that models which start with an adiabatic gradient can convect as a single cell for an appreciable time – up to $70 \cdot 10^6$ years – depending on the parameters of the system and the initial conditions. Whether the eventual breakdown of the convective system is real, or is due to numerical inaccuracies, cannot be definitely stated.

Steady-state solutions

Two typical results are shown in Fig.4 and 5 (Models 12 and 22, respectively). Their

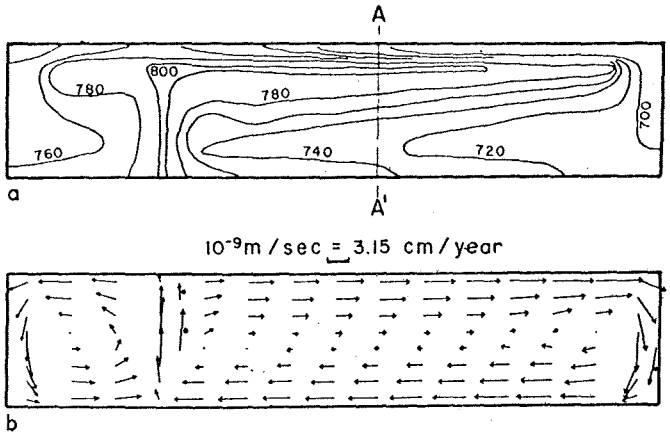

Fig.4. Temperature and velocity fields for Model 12. The arrows marked with a dot have been displaced for clarity.

main difference is that the radioactivity is lower than normal in the first one and normal in the second one (see Table I); as a consequence the theoretical surface heat flow (see below) is also below normal in the first one (44 mW m^{-2} = 1 H.F.U.) and normal in the second one (66 mW m^{-2} = 1.5 H.F.U.).

The parameters of both models are given in Table I. Shear heating is taken into account in both cases. By comparing results with and without shear heating it was found that the effect of the latter is to raise the temperature of the whole system by 45–49°C depending on the exact location. The absence of localized shear heating may appear remarkable, but is due to the fact that the dynamics of the present situation are quite different from those that prevail when a slab is moved through a stationary mantle.

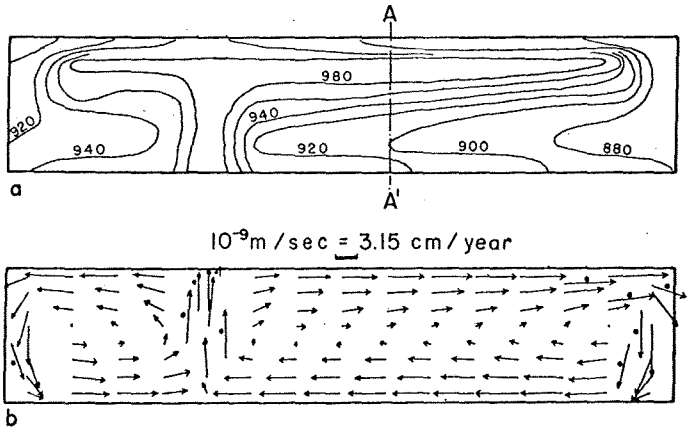

Fig.5. Temperature and velocity fields for Model 22. The arrows marked with a dot have been displaced for clarity.

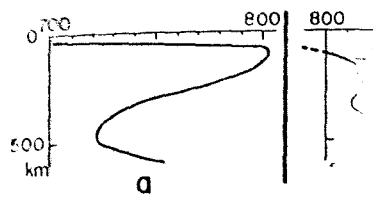

Fig.6. Temperature profile through sec... increase. b. With adiabatic temperature...

The asymmetry of the figures ...

The temperature profiles (Fig... of the low radioactivity of Model... When we take the effect of the a... ature rise in the upper 40 km is f... low this depth the temperature s...

This profile is markedly differ... the latter result from purely conc... the advective heat transfer excee... locity exceeds 0.03 cm/year (Cla... lem at hand. Instead, it is helpfu... ary layer, below which, as Jeffre... abatic. It is, perhaps, worth emp... the stated assumptions and the v... tial guess.

It appears likely that the effe... 100 km combine to cause partia... Below this depth the gradual rise... cosity. This picture conforms wi...

The temperature profiles wit... tively with those predicted by R... difference in Rayleigh numbers ... 10^7), and other differences, ma...

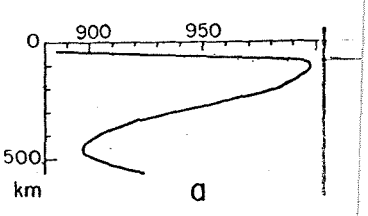

Fig.7. Temperature profile through ... increase. b. With adiabatic temperat...

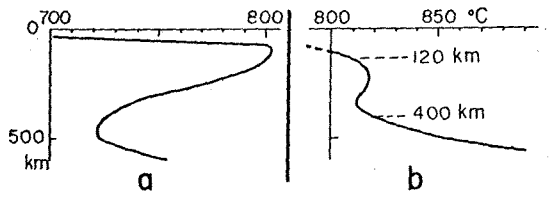

Fig.6. Temperature profile through section AA' of Fig.4 (Model 12). a. Without adiabatic temperature increase. b. With adiabatic temperature increase.

The asymmetry of the figures will be discussed later.

The temperature profiles (Fig.6 and 7) are similar in both cases, but, as a consequence of the low radioactivity of Model 12, its temperatures are probably lower than acceptable. When we take the effect of the adiabatic gradient into account, we see that a rapid temperature rise in the upper 40 km is followed by a slower rise to a depth of about 100 km. Below this depth the temperature stays essentially constant.

This profile is markedly different from those that are now classical; the reason is that the latter result from purely conductive solutions (e.g., Clark and Ringwood, 1964). Since the advective heat transfer exceeds the conductive heat transfer as soon as the vertical velocity exceeds 0.03 cm/year (Clark, 1969), a conductive solution is not relevant to the problem at hand. Instead, it is helpful to think of the top layer (lithosphere) as a thermal boundary layer, below which, as Jeffreys noted (1959, p.288) the temperature is essentially adiabatic. It is, perhaps, worth emphasizing that the temperatures everywhere result *only* from the stated assumptions and the values of the parameters; they are independent of the initial guess.

It appears likely that the effects of relatively high temperatures and low pressures near 100 km combine to cause partial melting and thus form a low velocity–low viscosity layer. Below this depth the gradual rise in pressure would correspond to a gradual increase in viscosity. This picture conforms with that proposed by Carter and Ave'Lallemant (1970).

The temperature profiles without the adiabatic gradient (Fig.5a and 6a) agree qualitatively with those predicted by Roberts (1967) for the roll and the down-hexagon; the large difference in Rayleigh numbers in his case ($R = 2.1 \cdot 10^4$) and in the present one ($R = 2.7 \cdot 10^7$), and other differences, make a quantitative comparison impossible.

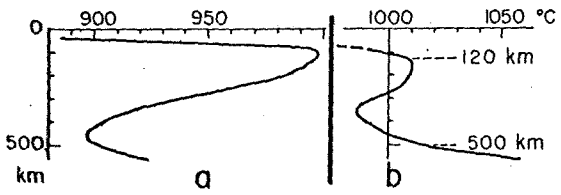

Fig.7. Temperature profile through section AA' of Fig.5 (Model 22). a. Without adiabatic temperature increase. b. With adiabatic temperature increase.

TABLE II

Theoretical (*TF*) and computed (*CF*) heat flow for Models 12 and 22 (in $W \cdot m^{-2} \cdot 10^{-3}$)

	TF	*CF*	Error (%)
Model 12	44	38	15
Model 22	65	59.5	9

The theoretical heat flow *TF* is given immediately (Table II) as:

$$TF = H \cdot D + F \tag{13}$$

where H and F have been defined previously, and D is the depth. The heat flow computed from the results (*CF*) (Table II) is:

$$CF = k \cdot \overline{T}_{i,s} / \tfrac{1}{2}\delta y$$

where $\overline{T}_{i,s}$ is the average temperature in the near-surface zone. If all the computations were exact, these two values should agree; the errors due to discretization, round-off, etc., cause them to differ. Table II shows that they differ by 15% in Model 12 and by only 9% in Model 22. This agreement is satisfactory considering the preliminary nature of the present work. It may be remarked that a comparison between the theoretical and the computed heat flow cannot be made for models in which the bottom temperature is fixed.

The lateral temperature difference is of the order of 100°C. In a restricted sense this may be viewed as the driving mechanism, although, in a larger sense, the system is, of course, driven by the presence of heat sources and heat sinks.

The surface velocities are reasonable, and increase downstream. This provides an unforeseen way out of the dilemma caused by the fact that, on the one hand the cooling of the upper 100 km cannot account for the whole heat flow, while, on the other hand, no heat can flow from below 100 km due to the absence of a thermal gradient. The system responds to this problem by constantly bringing hot material from below. This, of course, also explains the gentle rising of the streamlines in the downstream direction (i.e., the tilting upwards of the arrows). It is unclear whether this phenomenon has any geologic relevance; if it does, such an increase in velocity might perhaps take place in the low-velocity zone.

DISCUSSION

The temperatures found in Model 22 (which is closest to being realistic), are markedly lower than those generally proposed. Nevertheless, the temperature near 350 km (985°C) is in excellent agreement with that obtained from studies of phase changes. According to Ringwood (1972) the change from an olivine of pyrolite composition first to spinel and then to a β-phase takes place in a zone 27 km deep centered at 342 km if the temperature is 1000°C.

The gradual increase in temper
On the other hand the rapid temp
cause the necessary heat sources
rivatives by one-sided differences
proximation is satisfactory when
an extremum.

The asymmetry of the solution
solution in which the plume rises
stress-free conditions on the boun
been unsuccessful.

The grid taken for the comput
reason for this coarseness is the fa
rises rapidly with the number of
repeated using a 8 × 25 grid; altho
able, the temperatures near the e
Fig.4.

Another defect of the present s
tages: a minor one is the fairly po
rious one is less obvious: the tem
depth) is of the order of 900°C w
of the upper 20 km is only about
this cool material effectively vani
ceed as if the whole downgoing m
This effect is likely to be appreci

Other shortcomings are due to
isfactory solution is obtained in
plex one. It would, however, appe
be to alter the temperatures belo

CONCLUSIONS

All the evidence agrees with th
near the surface to approximately
depth the temperature changes li
km).

ACKNOWLEDGEMENTS

The advice and encouragemen
the Los Alamos Scientific Labora
ing Department, Rice University,
Production Research Laboratory

^{2} (in $W \cdot m^{-2} \cdot 10^{-3}$)

Error (%)
15
9

e II) as:

(13)

depth. The heat flow computed

one. If all the computations were
retization, round-off, etc., cause
lodel 12 and by only 9% in Mod-
inary nature of the present work.
tical and the computed heat flow
ure is fixed.
0°C. In a restricted sense this
rger sense, the system is, of course,

nstream. This provides an unfore-
ne one hand the cooling of the
ile, on the other hand, no heat
nal gradient. The system responds
below. This, of course, also ex-
n direction (i.e., the tilting up-
on has any geologic relevance;
lace in the low-velocity zone.

o being realistic), are markedly
perature near 350 km (985°C)
f phase changes. According to
mposition first to spinel and
d at 342 km if the temperature

The gradual increase in temperature in most of the bottom flow of the cell is expected. On the other hand the rapid temperature rise near the "plume" is physically impossible because the necessary heat sources do not exist. This rise is due to the approximation of derivatives by one-sided differences, i.e., to the "upwind" differences. Such a one-sided approximation is satisfactory when the function is monotonic, but not when it passes through an extremum.

The asymmetry of the solution is due to the same cause. Efforts to find a steady-state solution in which the plume rises at one side – because of the periodicity implied in the stress-free conditions on the boundaries, this would make for a symmetry solution – have been unsuccessful.

The grid taken for the computations is coarser than is desirable for good resolution. The reason for this coarseness is the fact that computer time – and the attendant expense – rises rapidly with the number of points in the grid. The computations for Model 22 were repeated using a 8 X 25 grid; although the fluctuations remained slightly larger than desirable, the temperatures near the end of the run differed only by about 25°C from these in Fig.4.

Another defect of the present solution is the constancy of δy. This has two disadvantages: a minor one is the fairly poor temperature resolution near the surface. The more serious one is less obvious: the temperature at the middle of the near-surface zone (37.5 km depth) is of the order of 900°C while the surface is at 0°C. Thus the average temperature of the upper 20 km is only about 450°C. When the current turns downwards the effect of this cool material effectively vanishes from the computations, i.e., the computations proceed as if the whole downgoing material was at the temperature of the center of the zone. This effect is likely to be appreciable.

Other shortcomings are due to the other simplifying assumptions. However, until a satisfactory solution is obtained in this simplified case, it seems unwise to attempt a more complex one. It would, however, appear that the effect of the phase change near 350 km will be to alter the temperatures below that depth.

CONCLUSIONS

All the evidence agrees with the fact that the temperature rises rapidly from near 0°C near the surface to approximately 900°C at 40 km and 1000°C near 120 km. Below this depth the temperature changes little until the first phase change is encountered (near 350 km).

ACKNOWLEDGEMENTS

The advice and encouragement received from Dr. Francis Harlow and his colleagues at the Los Alamos Scientific Laboratory, and of Dr. Berry Martin of the Chemical Engineering Department, Rice University, is gratefully acknowledged. Dr. Donald Peaceman, Esso Production Research Laboratory, Houston, Texas, made valuable suggestions. Dr. D.J.

Andrews sent me a preprint of his paper. Acknowledgement is made to the American Petroleum Institute and to the donors of the Petroleum Research Fund administered by the American Chemical Society for support of this research.

REFERENCES

Amsden, A.A. and Harlow, F.H., 1970. The SMAC method: a numerical technique for calculating incompressible fluid flows. *Los Alamos Sci. Lab., LA-4370, UC-32, Math. and Computers, TID-4500,* 85pp.

Andrews, D.J., 1972. Numerical simulation of sea-floor spreading. *J. Geophys. Res.*, 77: 6470–6481.

Bénard, H., 1901. Les tourbillons cellulaires dans une nappe liquide transportant de la chaleur par convection en régime permanent. *Ann. Chim. Phys., Ser. 7,* 23: 62–144.

Boussinesq, J., 1903. *Théorie analytique de la chaleur, v. 2.* Gauthier-Villars, Paris, 625pp.

Bullen, K.E., 1963. *An Introduction to the Theory of Seismology.* Cambridge Univ. Press, London, 381pp.

Carter, N.L. and Ave'Lallemant, H.G., 1970. High temperature flow of dunite and peridotite. *Geol. Soc. Am. Bull.*, 81: 2181–2202.

Clark, S.P., Jr., 1969. Heat conductivity in the mantle. In: P.J. Hart (Editor), *The Earth's Crust and Upper Mantle – Geophys. Monogr. 13.* Am. Geophys. Union, Washington, D.C., pp. 622–627.

Clark, S.P., Jr. and Ringwood, A.E., 1964. Density distribution and constitution of the Mantle. *Rev. Geophys.*, 2: 35–88.

Elsasser, W.M., 1966. Thermal structure of the upper mantle and convection. In: P.M. Hurley (Editor), *Advances in Earth Science.* M.I.T. Press, Cambridge, Mass., pp. 461–502.

Forsythe, G.E. and Wasow, W.R., 1960. *Finite-difference Methods for Partial Differential Equations.* Wiley, New York, N.Y., 444 pp.

Foster, T.D., 1969. Convection in a variable viscosity fluid heated from within. *J. Geophys. Res.*, 74: 685–693.

Greenspan, D., 1968. *Lectures on the Numerical Solution of Linear, Singular, and Nonlinear Differential Equations.* Prentice-Hall, London, 185 pp.

Griggs, D.T., 1972. The sinking lithosphere and the focal mechanism of deep earthquakes. In: E.C. Robertson (Editor), *The Nature of the Solid Earth.* McGraw-Hill, New York, N.Y., pp. 361–384.

Jeffreys, H., 1959. *The Earth.* Cambridge Univ. Press, London, 4th ed., 420 pp.

McKenzie, D.P., 1969. Speculations on the consequences and causes of plate motions. *Geophys. J.*, 18: 1–32.

McKenzie, D.P., 1972. Plate tectonics. In: E.C. Robertson (Editor), *The Nature of the Solid Earth.* McGraw-Hill, New York, N.Y., pp. 323–360.

Minear, J.W. and Toksöz, M.N., 1970. Thermal regime of a downgoing slab and new global tectonics. *J. Geophys. Res.*, 75: 1397–1419.

Peaceman, D.W., 1966. *Lecture notes on numerical solution of elliptic and parabolic partial differential equations.* Prepared for N.S.F. conference, Univ. of Colorado, Boulder, Colo.

Rayleigh, J.W., 1916. On convection currents in a horizontal layer fluid, when the higher temperature is on the under side. *Philos. Mag.*, 32: 529–546.

Ringwood, A.E., 1972. Mineralogy of the deep mantle: current status and future developments. In: E.C. Robertson (Editor), *The Nature of the Solid Earth.* McGraw-Hill, New York, N.Y., pp. 67–92.

Roberts, P.H., 1967. Convection in horizontal layers with internal heat generation: Theory. *J. Fluid Mech.*, 30: 33–49.

Shimazu, Y., Iriyama, J. and Urabe, T., 1967. Unsteady mantle convection. *J. Earth Sci., Nagoya Univ.*, 15: 81–98.

Torrance, K.E. and Rockett, J.A., 1969. Numerical study of natural convection in an enclosure with localized heating from below – creeping flow to the onset of laminar instability. *J. Fluid Mech.*, 36: 33–54.

Torrance, K.E. and Turcotte, D.L., 1
76: 1154–1161.
Torrance, K.E. and Turcotte, D.L., 1
tion to the mantle. *J. Fluid Mech.*
Tozer, D.C., 1967. Towards a theory
Earth's Mantle. Academic Press, L
Tritton, D.J. and Zarraga, M.N., 196
periments. *J. Fluid Mech.*, 30: 21–
Welch, J.E., Harlow, F.H., Shannon,
nique for solving viscous, incompr
Alamos Sci. Lab., LA-3425, UC-3

NOTE ADDED IN PROOF

Improved computations carried o
Houston and De Bremaecker, in pre
are generally correct. On the other h
if the viscosity is constant; much hig
cosity layer is at the top of the cell.

Houston, M.H. Jr., 1973. *Numerical diogenic Heating and Variable Vi*
Houston, M.H. Jr. and De Bremaeck
upper mantle.

s made to the American Pe-
n Fund administered by the

al technique for calculating in-
Math. and Computers, TID-4500,

eophys. Res., 77: 6470–6481.
ansportant de la chaleur par con-
4.
Villars, Paris, 625pp.
bridge Univ. Press, London,

f dunite and peridotite. *Geol. Soc.*

Editor), *The Earth's Crust and Up-*
gton, D.C., pp. 622–627.
onstitution of the Mantle. *Rev.*

vection. In: P.M. Hurley (Editor),
–502.
Partial Differential Equations.

m within. *J. Geophys. Res.*, 74:

Singular, and Nonlinear Differential

of deep earthquakes. In: E.C.
New York, N.Y., pp. 361–384.
., 420 pp.
of plate motions. *Geophys. J.*,

The Nature of the Solid Earth.

g slab and new global tectonics.

c and parabolic partial differential
lder, Colo.
uid, when the higher temperature

s and future developments. In:
-Hill, New York, N.Y., pp. 67–92.
at generation: Theory. *J. Fluid*

ection. *J. Earth Sci., Nagoya Univ.*,

convection in an enclosure with
nar instability. *J. Fluid Mech.*,

Torrance, K.E. and Turcotte, D.L., 1971a. Structure of convection cells in the mantle. *J. Geophys. Res.*, 76: 1154–1161.
Torrance, K.E. and Turcotte, D.L., 1971b. Thermal convection with large viscosity variations; application to the mantle. *J. Fluid Mech.*, 47: 113–125.
Tozer, D.C., 1967. Towards a theory of thermal convection in the mantle. In: T.F. Gaskell (Editor), *The Earth's Mantle*. Academic Press, London, pp. 325–353.
Tritton, D.J. and Zarraga, M.N., 1967. Convection in horizontal layers with internal heat generation. Experiments. *J. Fluid Mech.*, 30: 21–31.
Welch, J.E., Harlow, F.H., Shannon, J.P. and Daly, B.J., 1966. The MAC method; A computing technique for solving viscous, incompressible, transient fluid-flow problems involving free surfaces. *Los Alamos Sci. Lab., LA-3425, UC-32*, 146pp.

NOTE ADDED IN PROOF

Improved computations carried out here with both constant and variable viscosity (Houston, 1973; Houston and De Bremaecker, in preparation) have shown that our conclusions concerning temperatures are generally correct. On the other hand the convection cell should have an aspect ratio close to unity if the viscosity is constant; much higher aspect ratios occur in variable viscosity models if the high viscosity layer is at the top of the cell.

Houston, M.H. Jr., 1973. *Numerical Models of Free Convection in the Earth's Upper Mantle with Radiogenic Heating and Variable Viscosity.* Unpublished thesis, Rice University, Houston, Texas.
Houston, M.H. Jr. and De Bremaecker, J.Cl. (in preparation). Numerical models of convection in the upper mantle.